Korean J. Chem. Eng., 39(12), 3473-3481 (2022)
DOI: 10.1007/s11814-022-1221-1

pISSN: 0256-1115
eISSN: 1975-7220

Synthesis of fluorescent dye-embedded silica nanoparticles for vitamin D_3 detection using sandwich-like assay

Namhun Lee*, Seongsoo Kim*, Kwang-Ho Lee,†, Sang-Myung Lee*,***,†, and Dae-Won Lee*,†**

*Department of Chemical Engineering, Division of Chemical and Biological Engineering, Kangwon National University, Gangwon-do 24341, Korea
**Division of Mechanical & Biomedical, Mechatronics and Materials Science and Engineering, Kangwon National University, Gangwon-do 24341, Korea
***Department of Research and Development, Cantis Inc., Ansan-si, Gyeonggi-do 15588, Korea
(*Received 18 April 2022 • Revised 14 June 2022 • Accepted 3 July 2022*)

Abstract−This study devised and examined a sandwich-like assay for detecting vitamin D_3 dissolved in acetonitrile using fluorescent dye-embedded silica nanoparticles (AF647@SiNPs). First, AF647@SiNPs were synthesized *via* the modified Stöber method to embed the fluorescent dye molecules in the silicate network. Then, vitamin D_3 (sample) was immobilized using an azide linker on the magnetic nanoparticles (MNPs). The immobilized vitamin D_3 reacted with the antibody immobilized on the surface of AF647@SiNPs (Anti-VD_3@AF647@SiNPs). The vitamin D_3 concentration was calculated back using the fluorescence of the remaining unreacted Anti-VD_3@AF647@SiNPs. Finally, we examined how applying conditions of AF647@SiNPs influenced the measurement reliability: (1) the initial loading of AF647@SiNPs; (2) the antibody-labeling degree of AF647@SiNPs.

Keywords: Fluorescence Nanoparticles, Silica Nanoparticles, AF647 Dye, Vitamin D, Sandwich-like Assay

INTRODUCTION

Vitamin D (calcitriol) is a fat-soluble steroid hormone that is essential for maintaining bone, muscle, and immune health. In addition, vitamin D plays a principal role in regulating the calcium and phosphorous levels in the body. The primary forms of vitamin D are vitamin D_2 (ergocalciferol) and D_3 (cholecalciferol), which can be obtained from exogenous (food, supplement) or endogenous environment (on the skin after exposure to sunlight) [1-4]. It is generally known that both forms of vitamin D play similar roles in the body. However, vitamin D_3 is more effective than D_2 in raising the level of vitamin D. The deficiency of vitamin D_3 (<0.012 μg/mL) can lead to cancers, cardiovascular diseases, diabetes, and reduction of neurogenesis in the brain [5-7]. A high vitamin D_3 concentration (>0.15 μg/mL) is also toxic to the body, leading to hypercalcemia, recurrent vomiting, abdominal, muscle, or joint pain, and irregular heartbeat [8]. Therefore, it is essential to measure the vitamin D_3 concentration of a blood sample accurately and quickly.

There are many methods known for measuring vitamin D concentration, including radioimmunoassay (RIA) [9], electrochemical analysis [1,10,11], chemiluminescence immunoassay (CLIA) [12,13], and gas/liquid chromatography with mass spectrometry (GC/LC-MS) [14-17]. Some methods exhibit an excellent detection sensitivity and limit, but the most demand expensive equipment and lengthy analysis time [18,19].

In this study, we devised and examined the sandwich-like assay using fluorescent dye-embedded silica nanoparticles (F-SiNPs) for measuring vitamin D_3 concentration. The direct use of fluorescent dye molecules in bioassay applications has disadvantages, such as toxicity and photo-stability (photo-degradation and quenching). To overcome the disadvantages while maintaining the inherent properties of the fluorophore, it needs to embed or immobilize the fluorescent dye molecules over a supporting material [20,21]. The SiNPs, which could be easily prepared by the Stöber method, are widely used as immunoassay and catalyst support materials [22-24]. Also, they have various physical and chemical advantages as fluorophore support, such as biocompatibility, uniformity in size and morphology, and uncomplicated surface modification utilizing the chemistry of surface hydroxyl groups [25,26]. Therefore, F-SiNPs are widely utilized as the imaging probe or sensor material for molecular diagnosis related to drug and gene delivery [27,28]. González-García et al. reported that the dye-embedded organically modified SiNPs, conjugated with vitamin D_3, showed a high affinity to human serum albumin (HSA) [29]. The affinity of the vitamin D_3 conjugated on SiNPs to HSA was in the same order of magnitude as free vitamin D_3. The authors stressed that because HSA is a well-known targeting agent for tumor cells, the vitamin D_3-conjugated SiNPs could be exploited as potential drug delivery agents. Based on this, we considered it possible to detect vitamin D_3 by utilizing the reaction of vitamin D_3 with its antibody immobilized on the SiNP surface. Furthermore, vitamin D_3 concentration can be quantified using fluorescent dye-embedded SiNPs (F-SiNPs) and fluorescence techniques. To realize this, we devised a procedure (*i.e.*, a sandwich-like assay) to immobilize vitamin D_3 and its antibody on F-SiNP and its counterpart support material (magnetic nanoparticle).

†To whom correspondence should be addressed.
E-mail: khmhlee@kangwon.ac.kr, smlee@cantis.co.kr, stayheavy@kangwon.ac.kr

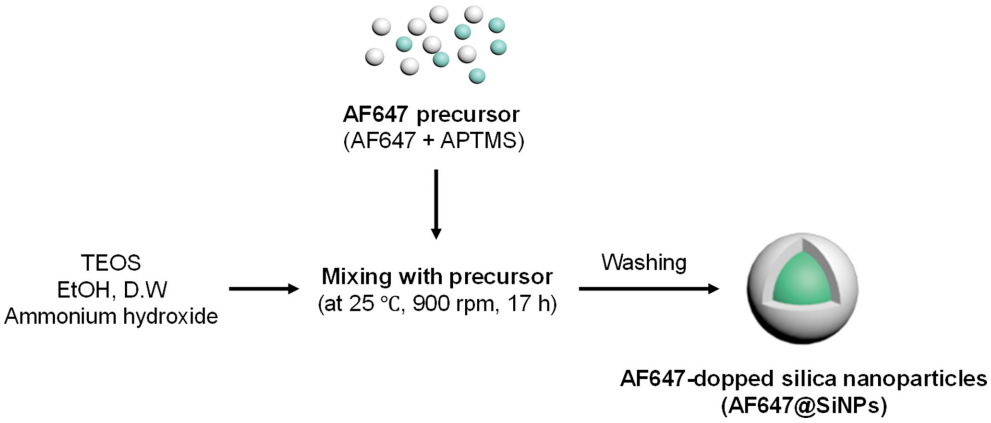

Fig. 1. The synthesis of AF647@SiNPs.

We modified the Stöber method to synthesize the fluorescent dye-embedded silica nanoparticles. We used Alex Fluor™ 647 dye (AF647) with excitation/emission maxima at 650/667 nm as the fluorescent dye. AF647 was coupled with (3-aminopropyl)trimethoxysilane (APTMS), then mixed with the silicate precursor solution. The Stöber synthesis was then performed, producing the AF647-embedded silica nanoparticles functionalized with amines on the surface (AF647@SiNPs). We optimized the synthesis procedure of AF647@SiNPs to improve the photoluminescence activity. Then, the vitamin D_3 antibody was immobilized on AF647@SiNPs, and coupled with the vitamin D_3 captured by the surface-modified magnetic nanoparticles. A procedure for fluorescence analysis was devised, and the optimal applying conditions of AF647@SiNPs were determined for measuring vitamin D_3 concentration, by which we could finally establish the sandwich-like assay.

EXPERIMENTS

1. Materials

The following materials were purchased from Sigma-Aldrich (USA): (3-aminopropyl)trimethoxysilane (APTMS, ≥98%), N-hydroxysuccinimide (NHS, ≥98%), ethyl(dimethylaminopropyl) carbodiimide (EDC, ≥98%), 2-(N-morpholino)ethanesulfonic aicd (MES, ≥99%), dimethyl sulfoxide anhydrous (DMSO, ≥99.9%), ethyl alcohol (EtOH, ≥99.5%), tetraethyl orthosilicate (TEOS, ≥98%), (3-aminopropyl)triethoxysilane (APTES, ≥98%), bovine serum albumin (BSA, ≥96%), 4-phenyl-1,2,4-triazole-3,5-dione azide (PTAD-azide, ≥95%), 1,3,-dibromo-5,5-dimethylhydantoin (DBDMH, ≥98%), acetonitrile anhydrous (ACN, ≥99.8%), ammonium hydroxide (28-30%). Dibenzocyclooctyne-polyethylene glycol-amine (DBCO-PEG-NH_2, PG2-AMDB-2k) and hyaluronic acid (HA, 10 kDa) were purchased, respectively, from Nanocs (USA) and GL Biochem (China). 25-Hydroxyl vitamin D_3 and its antibody were purchased, respectively, from Cayman Chemical (USA) and Antibodies-Online (USA). Magnetic nanoparticles (MNPs, -COOH, Dynabeads M-270) and Alex Fluor™ 647 dye (AF647) were purchased from Thermo Fisher Scientific (USA). All materials were used without further purification.

2. Synthesis of AF647@SiNPs

First, 50 μL of AF647 solution (2 mg/mL, DMSO) was mixed immediately with 50 μL of APTMS solution (20-200 μM, DMSO) to prepare the AF647 precursor solution. And then, a TEOS solution was prepared for Stöber synthesis of silica nanoparticles. A standard TEOS solution was prepared by mixing 1 mL of TEOS, 1.88 mL of deionized water (D.W), 0.32 mL of ammonium hydroxide (28-30%), and 17.6 mL of ethanol (solvent). The solvent effect on Stöber synthesis was examined using methanol/ethanol mixture solvents in various molar ratios (0/100, 10/90, 30/70, 50/50, or 100/0). The AF647 precursor solution was injected into the TEOS solution at various timings: (1) 0 min: right at the moment when a TEOS solution was prepared (single injection); (2) 30 min: 30 minutes after a TEOS solution was prepared (single injection); 0+30: injecting half of the precursor at 0 min and then the other half at 30 min (half-half injection); (4) 60 min (single injection); (5) 0+60 min (half-half injection). The mixed solution was stirred at 900 rpm for 2-13 hours. The precipitates (AF647@SiNPs) were collected and washed five times with ethanol.

Next, the washed AF647@SiNPs were re-dispersed over 20 mL of ethanol, to which 20 μL of APTES was injected to functionalize the surface of AF647@SiNPs with amine groups. The stirring continued for 12 hours to complete the amine functionalization, and then the amine-functionalized AF647@SiNPs were collected (AF647@SiNPs-NH_2). The overall procedure for preparing AF647@SiNPs is illustrated in Fig. 1.

3. Immobilization of Vitamin D_3 Antibody over AF647@SiNPs (Anti-VD_3@AF647@SiNPs)

20 mg of AF647@SiNPs-NH_2 (dispersed over 100 mL of MES buffer (10 mM, pH 6.0)) was reacted with 2 mg of HA for three hours to obtain the carboxylic acid-modified AF647@SiNPs (AF647@SiNPs-COOH). 1 mL of the dispersed AF647@SiNPs-COOH slurry was labeled by 100 μL of vitamin D_3 antibody (100, 250, or 500 μg/mL) for two hours *via* EDC/NHS coupling reaction (50 μL of 0.26 mM EDC (MES) and 50 μL of 0.43 mM EDC (MES)). The antibody-labeled AF647@SiNPs were obtained (Anti-VD_3@AF647@SiNPs) and then coated with 0.1 w/v% of BSA to block any non-specific protein binding. All the steps were performed at room temperature (25 °C).

4. Preparation of Vitamin D_3 Samples and Immobilization of Vitamin D_3 over Magnetic Nanoparticles (Vitamin D_3@MNPs)

A known concentration of vitamin D_3 was dissolved in a pure ACN or ACN/D.W (60 : 40 in volume ratio) solvent to prepare a

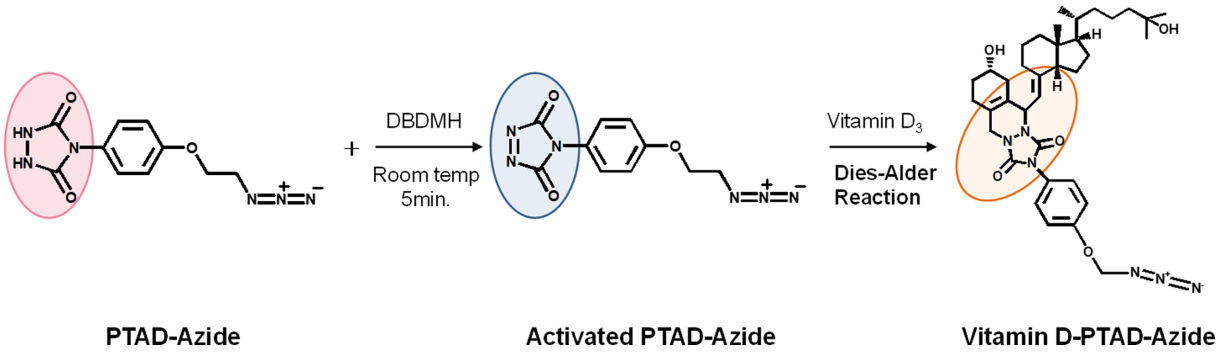

Fig. 2. The activation of PTAD-azide and its conjugation with vitamin D_3.

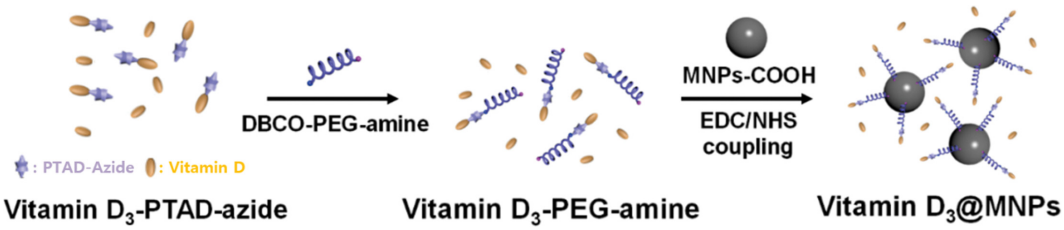

Fig. 3. The procedure for vitamin D_3 immobilization over MNPs (vitamin D_3@MNPs).

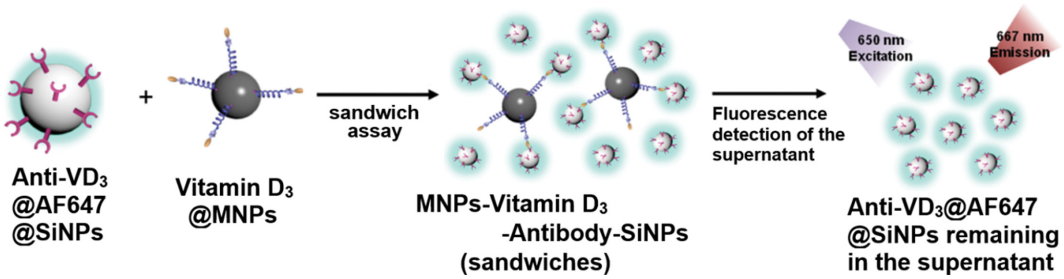

Fig. 4. The sandwich-like assay using AF647@SiNPs and MNPs.

vitamin D_3 sample (volume=20 μL, concentration=0.01, 0.025, 0.05, 0.075, and 0.1 μg/mL).

We used PTAD-azide as a link molecule to immobilize vitamin D_3 (Fig. 2): First, 10 μL of PTAD-azide (20 mM, ACN or ACN/D.W (60/40 v/v %) was activated using 10 μL of DBDMH (20 mM, ACN or ACN/D.W (60/40 v/v %)) for 5 min at 25 °C (Fig. 2). Then, vitamin D_3 in a sample (20 μL, various concentrations) was conjugated with the activated PTAD-azide (20 μL, 20 mM) *via* Diels-Alder reaction at 25 °C for 1-10 min (Fig. 2). The conjugation product was analyzed using high-performance liquid chromatography (HPLC, YL9100, Young Lin). 20 μL of a sample was injected and separated on YL C18-4D analytical column (4.6×150 mm, 5.0 μm, Stationary phase: C18, ODS). The mobile phase (ACN or ACN/D.W (60/40 v/v %)) flowed at 1 mL/min in an isocratic elution mode. The separated species were detected by a UV detector (264 nm).

The PTAD-azide-conjugated vitamin D_3 was reacted with 20 mM of DBCO-PEG-NH_2 at 37 °C for 2 hours using click chemistry (DBCO-azide conjugation). Next, the 100 μL of the DBCO-azide conjugation product (Vitamin D_3-PEG-NH_2) was reacted with 100 μL of MNPs (5 mg/mL, MES buffer (10 mM, pH 6.0)) using EDC/NHS coupling reagent (50 μL of 0.26 mM EDC (MES) and 50 μL of 0.43 mM EDC (MES)) at 25 °C with stirring at 800 rpm for two hours. The final product, Vitamin D_3@MNPs, was collected and washed two times with 10 mM PBS buffer (pH 6.0). To block non-specific protein bindings, the Vitamin D_3@MNPs were treated with 0.1 w/v% of BSA for 0.5 hours and washed two times with PBS buffer. The overall procedure for preparing Vitamin D_3@MNPs is illustrated in Fig. 3.

5. Measurement of Vitamin D_3 Concentration: Sandwich-like Assay

First, the fluorescence intensity of 100 μL of Anti-VD_3@AF647@SiNPs was measured using a fluorescence spectrometer (Fluoro-Mate FS-2, SCINCO, Korea). Next, 100 μL of Anti-VD_3@AF647@SiNPs was reacted with 100 μL of Vitamin D_3@MNPs (50 μg/mL) at 35 °C for 1 hour, by which the vitamin D_3-antibody conjugate was sandwiched between SiNPs and MNPs (hence, 'sandwich-like assay') The SiNPs-Vitamin D_3-MNPs sandwiches were collected using an ultra-magnet, and the fluorescence intensity (650/667 nm) of the unreacted Anti-VD_3@AF647@SiNPs remaining in the supernatant was measured. The result was subtracted from the

fluorescence intensity of 100 μL of Anti-VD_3@AF647@SiNPs measured in advance, by which we could calculate back the vitamin D_3 concentration of the sample. The procedure of the sandwich-like assay is summarized in Fig. 4.

6. Characterization of AF647@SiNPs

The morphology of the synthesized AF647@SiNPs and final sandwich-like assay products were observed by TEM (LEO 912AB Omega, Zeiss, Germany). The dynamic light scattering (DLS) was analyzed using a particle size analyzer (ELSZ-2000, Otsuka, Japan).

RESULTS AND DISCUSSION

1. Synthesis of AF647@SiNPs

We investigated how the synthesis conditions affect the photoluminescence activity of AF647@SiNPs. We first examined the effects of the composition and mixing time of the AF647 precursor solution. Fig. 5(a) shows that the increase of APTMS content in AF647 precursor solution increased the fluorescence intensity of AF647@SiNPs. However, because it also increased the total mass of precipitates, it was reasonable to reevaluate the photoluminescence activity in weight-normalized fluorescence intensity (the fluorescence intensity per a mass of AF647@SiNPs). The normalized intensity showed a decreasing trend as APTMS enriched in AF647 precursor solution (Fig. 5(b)). In addition, the fluorescence intensity decreased gradually with the increase of time allowed for the mixing of APTMS and AF647 solutions (Fig. 5(c)). It was surmised that the frequent contact with APTMS chemically deactivates AF647 or hinders the embedment of AF647 molecules over the silica network. Hence, the AF647 precursor solutions were prepared using the lowest APTMS concentration we had tried (1×, *i.e.*, 20 μM) and applied to the Stöber process immediately (*i.e.*, 0 hour) as it was prepared.

Next, we examined the effect of methanol/ethanol solvent in the Stöber process on the size and morphology of the AF647@SiNPs. The TEM images in Fig. 6 show that the size of AF647@SiNPs decreased with the increase of methanol content in a solvent. It is probably because the hydrolysis and condensation of TEOS are relatively fast under methanol solvent, leading to the formation of tiny silicate seeds [30]. The precipitates were perfectly spherical if

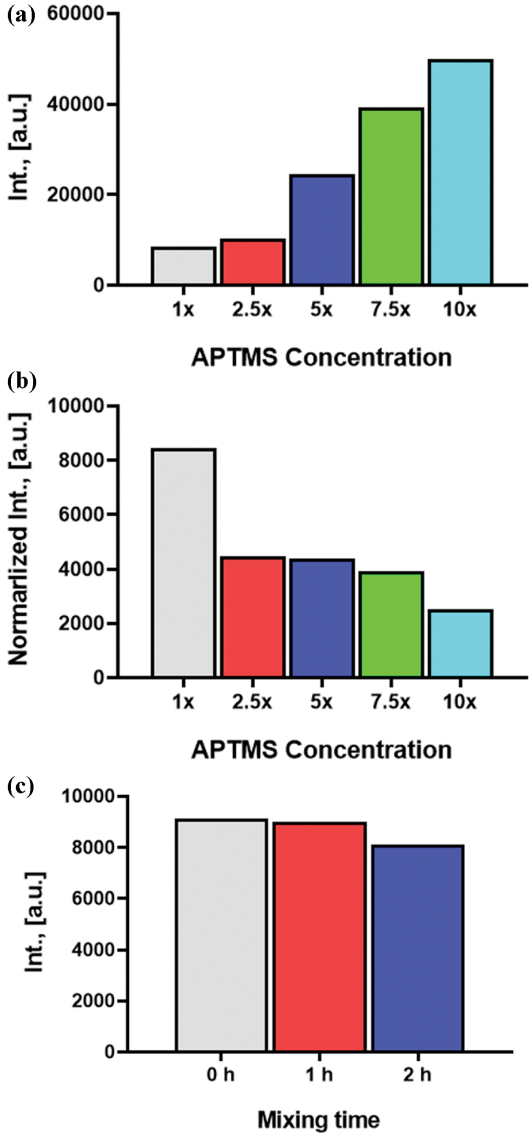

Fig. 5. The fluorescence intensity (672 nm) of AF647@SiNPs synthesized with changing the preparation conditions for 'AF647 precursor solution': (a) APTMS concentration (1×=20 μM, 10×=200 μM), (b) Replot of (a) with weight-normalized intensity, (c) AF647-APTMS mixing time (0-2 h).

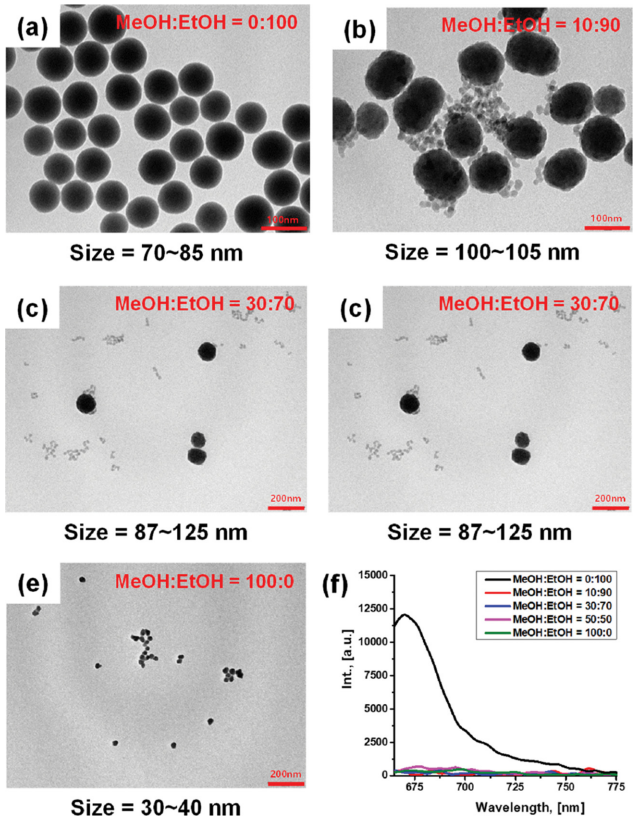

Fig. 6. TEM images of AF647@SiNPs synthesized under different methanol/ethanol solvent: the molar ratio of methanol/ethanol =(a) 0/100, (b) 10/90, (c) 30/70, (d) 50/50, (e) 100/0, and (f) the fluorescence intensity of AF647@SiNPs (a)-(e).

the Stöber synthesis was performed under pure ethanol (Fig. 6(a)), but the morphology became ellipsoidal if the synthesis was performed under a methanol-ethanol mixture or pure methanol (Fig. 6(b)-(e)). Fig. 6(f) shows that the AF647@SiNPs prepared under pure ethanol were exceptionally high in fluorescence intensity, whereas the intensity was drastically reduced for the AF647@SiNPs prepared under methanol-containing solvents. It is surmised that the self-quenching effect became intensified as the fluorescent molecules (AF647) enriched in an SiNP due to the small size of the AF647@SiNPs obtained under a methanol-containing solvent [31].

We changed the amount of TEOS (0.1, 0.5, and 1.0 mL) for Stöber synthesis and examined its effect on the precipitate size of AF647@SiNPs (Table 1). Although the TEOS amount changed five or ten times, the average particle size of AF647@SiNPs (based on DLS analysis) changed only 2-5%, maintaining the size around ~110 nm. It implies that although the Stöber synthesis proceeds with the silicon precursors mixed with organic fluorescent molecules, it could still obtain SiNPs of uniform size [32].

Table 1. Average particle size of AF647@SiNPs prepared using different amount of TEOS

TEOS amount (mL)	0.1	0.5	1.0
Average particle size (nm)	107.3±6.4	109.4±13.8	112.4±15.7

※ Measured by DLS analysis

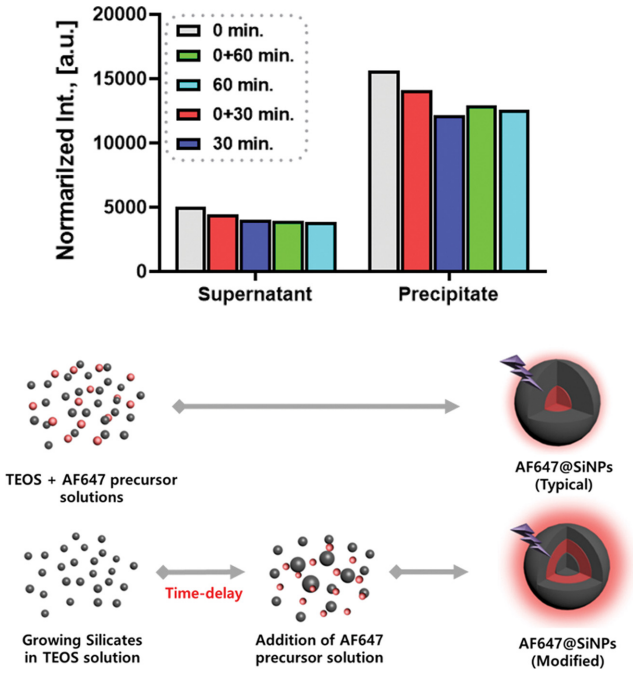

Fig. 7. The fluorescence intensity (672 nm) of AF647@SiNPs according to the injection method of AF647 precursor into TEOS solution; 0 min=injected the precursor all at once right at the moment when a TEOS solution was prepared (single injection); 30 (or 60) min=injected the precursor all at once, passing 30 (or 60) minutes after a TEOS solution was prepared (single injection); 0+30 (or 0+60) min=injected half of the precursor at 0 min and then the other half at 30 (or 60) min (half-half injection).

Fig. 7(a) presents the effects of the injection method and timing of AF647 precursor into TEOS solution on the photoluminescence activity of AF647@SiNPs. We anticipated that the fluorescence intensity would increase if the injection timing were delayed because AF647 would conjugate with moderately grown silicates and consequently be placed closer to the outer periphery of the SiNPs. However, the fluorescence intensity of the AF647@SiNPs decreased as the injection timing was delayed to 30 and 60 min. The supernatants of precipitates (AF647@SiNPs) showed a slightly decreasing but similar fluorescence intensity with the delay of injection timing, which means the amount of AF647 conjugated with SiNPs was similar regardless of the injection timing and method. Meanwhile, the half-half injection seemed to be advantageous over the single injection method concerning the photoluminescence activity of the precipitate: The fluorescence intensity of 0+30 and 0+60 min precipitates was higher than that of 30 and 60 min precipitates, respectively. Nevertheless, the fluorescence intensity of the 0+30 and 0+60 min precipitates was still lower than that of the 0 min sample. The variation of the injection timing also influenced little the particle size of AF647@SiNPs, as shown in the TEM images given in Fig. 8. Therefore, it is supposed that the AF647 precursor was conjugated with silicate seeds or growing silicates immediately as it was injected into the TEOS solution. The distribution of AF647 at the outer periphery of AF647@SiNPs did not improve the photoluminescence activity. Contrary to expectations, it seems to deteriorate the photoluminescence activity of AF647@SiNPs, similarly to the self-quenching effect [31]. Therefore, the best way to achieve the highest photoluminescence activity was to inject the AF647 precursor all at once right when a TEOS solution was prepared.

Finally, the prepared AF647@SiNPs were very stable in aqueous media (Fig. 9). The photoluminescence activity and average particle size (DLS analysis) did not change appreciably for 30 days regardless of whether the storage temperature was 4 or 25 °C.

As a final step, the AF647@SiNPs were labeled by vitamin D_3 antibody (Anti-VD_3@AF647@SiNPs). We used the antibody solutions in different concentrations (100, 250, and 500 μg/mL) for this procedure. We thereby tried to find the most appropriate surface antibody concentration of Anti-VD_3@AF647@SiNPs to measure 0.01-0.1 μg/mL vitamin D_3. The results will be presented and discussed later in section 3.3.

2. Immobilization of Vitamin D_3 over MNPs (Preparation of Vitamin D_3@MNPs)

Next, we immobilized vitamin D_3 on the magnetic nanoparticles (Vitamin D_3@MNPs). The immobilized vitamin D_3 would be coupled with the antibody molecule immobilized on AF647@SiNPs (Anti-VD_3@AF647@SiNPs) to obtain an MNPs-Vitamin D_3-Antibody-SiNPs adduct used for the sandwich-like assay.

First, the diene group of vitamin D_3 was conjugated with activated PTAD-azide *via* Diels-Alder reaction (Fig. 2) [33-35]. The conjugation was performed in a pure ACN or ACN/D.W (60/40 v/v%) solvent for 1, 3, or 10 min. In HPLC analysis, the bare, unconjugated vitamin D_3 was detected as an innate peak at 32 min (Fig. 10: *black* line). The conjugated vitamin D_3 was detected at around 20 min (Fig. 10: *red*, *blue*, *pink*, and *green* lines). The peak was more intense when the conjugation was conducted in the ACN/

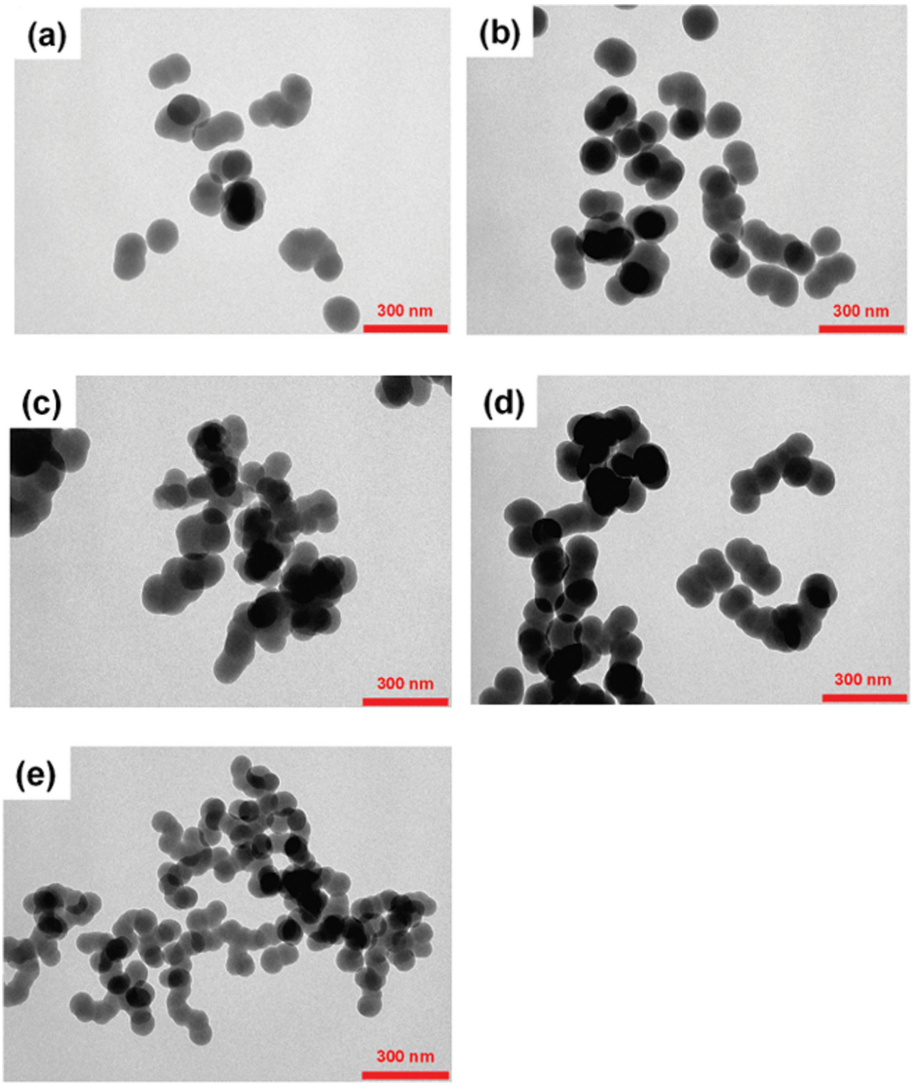

Fig. 8. TEM image of AF647@SiNPs synthesized with changing the injection method of AF647 precursor into TEOS solution: (a) 0 min, (b) 0+30 min, (c) 30 min, (d) 0+60 min, (e) 60 min.

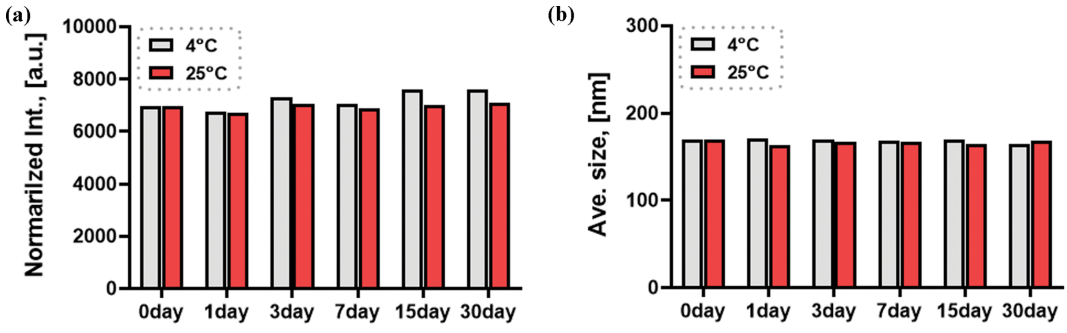

Fig. 9. Stability test of AF647@SiNPs for 30 days: (a) Photoluminescence activity, (b) Average particle size (DLS analysis).

D.W media, and the peak was detected, although only one minute was allowed for the reaction. It implies the Diels-Alder reaction occurs so fast in the ACS/D.W media that it completes within a minute. It also means the PTAD-azide-conjugated vitamin D_3 is stable in the presence of water, which could be an advantage in the analysis of vitamin D_3 mixed with water because vitamin D_3 is unstable in an aqueous media [36].

The azide group of conjugated vitamin D_3 reacted with the cyclooctyne group of DBCO-PEG-NH_2, generating a triazole link to form the DBCO-azide conjugation product (Vitamin D_3-PEG-

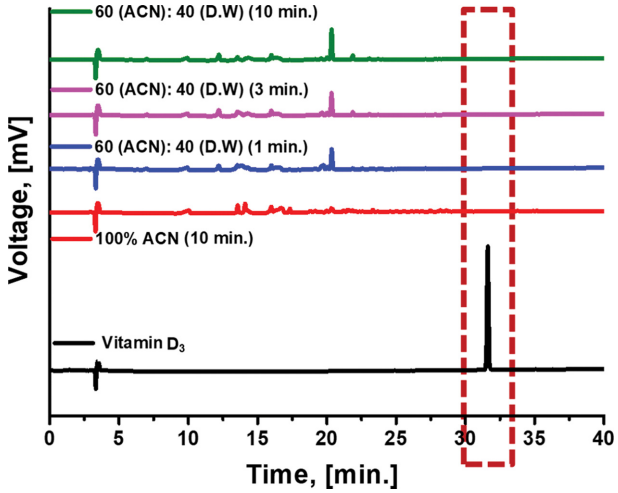

Fig. 10. HPLC analysis results of vitamin D_3 (*black line*) and PTAD-azide-conjugated vitamin D_3 (*red, blue, pink,* and *green lines,* which were different in the solvent where vitamin D_3 was conjugated with PTAD-azide linker and the time allowed for the conjugation.).

NH_2). Then, the amine group of Vitamin D_3-PEG-NH_2 reacted with the carboxylic acid group of MNPs (-COOH) *via* EDC-NHS coupling, by which we could immobilize vitamin D_3 on the MNP surface, finally obtaining Vitamin D_3@MNPs (Fig. 3), which were demanded in the sandwich-like assay.

3. Measurement of Vitamin D_3 Concentration

Fig. 11 shows the measurement results of vitamin D_3 samples (0.01-0.1 μg/mL) with using Anti-VD_3@AF647@SiNPs in different loading amount (5, 10, 25, 50 mg/mL). Because we measured the fluorescence of the free surplus Anti-VD_3@AF647@SiNPs, which remained in the liquid after completion of coupling with vitamin D_3@MNPs (Fig. 4), the fluorescence intensity always decreased with the increase of initial vitamin D_3 concentration regardless of the test conditions. The plot between fluorescence intensity and vitamin D_3 concentration showed a good linearity (R^2=0.99) when applying relatively low loading of AF647@SiNPs (5 mg/mL: Fig. 11(a)). As the loading of AF647@SiNPs increased to 10, 25, 50 mg/mL, the linearity became poor (R^2=0.7, 0.8: Fig. 11(b) and (c)) or the slope of the plot became too low to distinguish the vitamin D_3 concentration of the samples (Fig. 11(d)). Therefore, we concluded that using 5 mg of AF647@SiNPs per mL of the entire test liquid is the most appropriate for measuring 0.01-0.1 μg/mL of vitamin D_3.

Next, we examined how the antibody labeling of AF647@SiNPs influences the measurement of vitamin D_3 concentration. We had presumed the presence of the optimal surface antibody concentration of the Anti-VD_3@AF647@SiNPs in capturing vitamin D_3 because an antibody deficiency would result in the incomplete cap-

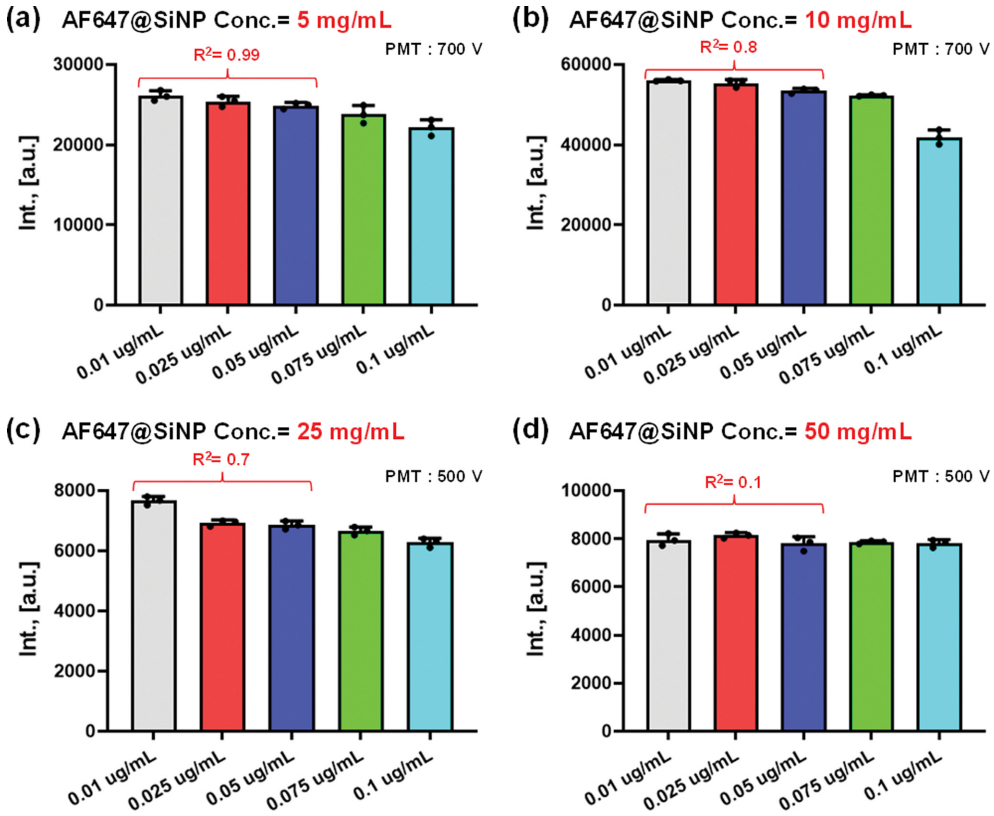

Fig. 11. The sandwich-like assay test results using AF647@SiNPs (more specifically, Anti-VD_3@ AF647@SiNPs) in different loading amount: (a) 5 mg/mL, (b) 10 mg/mL, (c) 25 mg/mL, and (d) 50 mg/mL: For the (c) and (d) cases, the PMT value was lowered from 700 to 500 V because the fluorescence intensity had exceeded the detection limit of spectrometer as the concentration AF647@SiNPs became high (25 and 50 mg/mL).

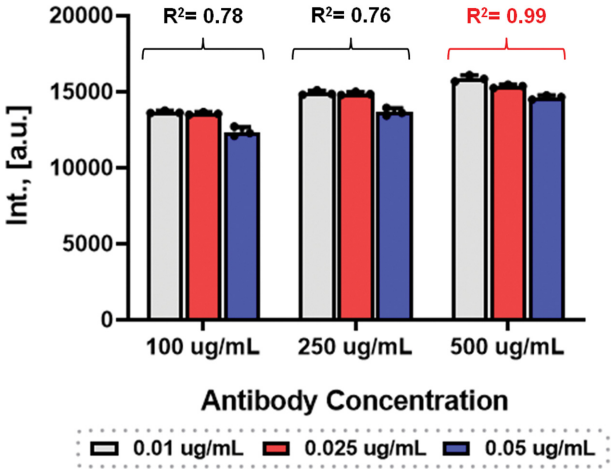

Fig. 12. The sandwich-like assay test results using Anti-VD_3@AF647@SiNPs, which were prepared with the vitamin D_3 antibody solution in different concentration (100, 250, and 500 μg/mL).

ture of vitamin D_3, while an antibody excess would quench (or screen) the photoluminescence activity of AF647@SiNPs. Therefore, to examine antibody effects, we prepared three Anti-VD_3@AF647@SiNPs using the antibody solutions in different concentrations (100, 250, and 500 μg/mL).

As presented in Fig. 12, the detection results of 0.025 and 0.05 μg/mL vitamin D_3 were discernible using any of three Anti-VD_3@AF647@SiNPs. However, the detection of vitamin D_3 in the lower concentration range (0.01 and 0.025 μg/mL) was acceptable only when using the highest-level antibody-labeled AF647@SiNPs (500 Anti-VD_3 μg/mL). Consequently, its overall determination coefficient (R^2) was 0.99 in the plot between fluorescence intensity and vitamin D_3 concentration. It was supposed that although we had labeled AF647@SiNPs using the antibody solution of the highest concentration available (500 μg/mL), the quenching effect of the antibody was not significant. On the other hand, the use of low-level antibody-labeled AF647@SiNPs (100 and 250 Anti-VD_3 μg/mL) did not discern 0.01 and 0.025 μg/mL, which resulted in poor overall linearity (R^2=0.78, 0.76). It was surmised that the vitamin D_3 concentration gradient could be relatively small in the external diffusion layer due to the scarcity of antibodies on the surface, making the capture of vitamin D_3 limited by diffusion resistance.

CONCLUSIONS

A vitamin D_3 detection method was devised based on the sandwich-like assay and fluorescence analysis. The fluorescent dye-embedded SiNPs (AF647@SiNPs) were successfully synthesized using the Stöber method, which was slightly modified by using the TEOS solution mixed with AF647 precursor (AF647+APTMS) for precipitation. The AF647 precursor should be carefully prepared and applied to obtain the best (normalized) photoluminescence activity of the precipitates (AF647@SiNPs). The AF647 solution (2 mg/mL) was mixed with the APTMS solution (20 μM) in a 1 : 1 volume ratio, and the mixture had to be injected onto the TEOS solution as soon as it was prepared. The half-half injection and the delay of injection timing were not effective in improving the photoluminescence activity of the AF647@SiNPs precipitates. AF647@SiNPs presented better photoluminescence activity when synthesized under pure ethanol solvent than a methanol-containing solvent. The prepared AF647@SiNPs maintained dispersion stability over aqueous media for 30 days at the storage temperature of 4 and 25 °C.

Vitamin D_3 in a sample was immobilized in the state conjugated with PTAD-azide over MNPs and then labeled with the antibody immobilized over AF647@SiNPs. The adducts (MNPs-Vitamin D_3-Antibody-SiNPs) were removed, the fluorescence of the remaining unlabeled AF647@SiNPs was measured, by which we could calculate back the vitamin D_3 concentration of the sample. The surface antibody concentration of Anti-VD_3@AF647@SiNPs was crucial for the measurement reliability. We could achieve an acceptable detection response between vitamin D_3 concentration and fluorescence intensity using the highest-level antibody-labeled AF647@SiNPs (500 Anti-VD_3 μg/mL). Using 5 mg of AF647@SiNPs per mL of the entire test liquid was the most adequate for measuring 0.01-0.1 μg/mL of vitamin D_3.

ACKNOWLEDGEMENT

This research was supported by Basic Science Research Program through the National Research Foundation of Korea (NRF) funded by the Ministry of Science & ICT (MSIT) (NRF-2016R1A5A1009592).

REFERENCES

1. F. H. Cincotto, T. C. Canevari and S. A. S. Machado, *Electroanalysis*, **26**(12), 2783 (2014).
2. E. Kasalova, J. Aufartova, L. K. Krcmova, D. Solichova and P. Solich, *Food Chem.*, **171**, 177 (2015).
3. E. J. Dufek, B. Ehlert, M. C. Granger, T. M. Sandrock, S. L. Legge, M. . Herrmann, A. W. Meikle and M. D. Porter, *Analyst*, **135**(11), 2811 (2010).
4. A. M. Wallace, S. Gibson, A. de la Hunty, C. Lamberg-Allardt and M. Ashwell, *Steroids*, **75**(7), 477 (2010).
5. S. Kia, M. Fazilati, H. Salavati and S. Bohlooli, *RSC Adv.*, **6**(38), 31906 (2016).
6. X. He, P. Jiang, Y. Xue, W.-Y. Zhu, Y. Deng, M. Yan, H.-D. Li, R.-L. Dang and M.-M. Tang, *Methods*, **8**(11), 2400 (2016).
7. H. Dobnig, S. Pilz, H. Scharnagl, W. Renner, U. Seelhorst, B. Wellnitz, J. Kinkeldei, B. Boehm, G. Weihrauch and W. Maerz, *Arch. Intern. Med.*, **12**, 1340 (2008).
8. K.Galior, S. Grebe and R. Singh, *Nutrients*, **10**(8) 953 (2018).
9. B. W. Hollis, J. Q. Sandra, S. R. Selvaag, J. D. Lorenz and J. L. Napoli, *Clin. Chem.*, **39**, 529 (1993).
10. D. Chauhan, R. Kumar, A. K. Panda and P. R. Solanki, *J. Mat. Res. Tech.*, **8**(6), 5490 (2019).
11. D. Chauhan, P. K. Gupta and P. R. Solanki, *Mater. Sci. Eng. C.*, **93**, 145 (2018).
12. M. K. Koivula, N. Matinlassi, P. Laitinen and J. Risteli, *Clin. Lab.*, **59**(3-4), 397 (2013).

13. S. Lee, J.-H. Kim., S.-A. Kim, Y.-S. Sun, A. Lee, S.-J. Park, Y.-T. Kim, K.-R. Lee and Y.-J. Kim, *Ann. Clin. Lab. Sci.*, **46**, 645 (2016).
14. M. J. Bogusz, E. Al Enazi, M. Tahtamoni, J. A. Jawaad and M. A. Tufail, *Clin. Biochem.*, **44**(16), 1329 (2011).
15. R. D. Coldwell, D. J. Trafford, M. J. Varley, D. N. Kirk and H. L. J. Makin, *Clinica Chimica Acta*, **180**, 157 (1989).
16. G. D. Carter and J. C. Jones, *Ann. Clin. Biochem.*, **46**, 79 (2009).
17. A. P. D. Leenheer and A. A. Cruyl, *Anal. Biochem.*, **91**, 293 (1978).
18. P. B. Luppa, C. Muller, A. Schlichtiger and H. Schlebusch, *Trends. Anal. Chem.*, **30**(6), 887 (2011).
19. R. F. Louie, Z. Tang, D. G. Shelby and G. J. Kost, *Lab. Med.*, **31**, 402 (2000).
20. E. Herz, H. Ow, D. Bonner, A. Burns and U. Wiesner, *J. Mater. Chem.*, **19**(35), 6341 (2009).
21. H. Ow, D. R. Larson, M. Srivastava, B. A. Baird, W. W. Webb and U. Wiesner, *Nano Lett.*, **5**(1), 113 (2005).
22. F. Hao, J. Zheng, D. Ouyang, W. Xiong, P. Liu and H. Luo, *Korean J. Chem. Eng.*, **38**(4), 736 (2021).
23. S. B. Jo, H. J. Chae, T. Y. Kim, J.-I. Baek, D. Ragupathy, S. C. Lee and J. C. Kim, *Korean J. Chem. Eng.*, **37**(12), 2317 (2020).
24. S. Saleh, A. Younis, R. Ali and E. Elkady, *Korean J. Chem. Eng.*, **36**(4), 529 (2019).
25. S. Liang, C. L. John, S. Xu, J. Chen, Y. Jin, Q. Yuan, W. Tan and J. X. Zhao, in *Advanced fluorescence reporters in chemistry and biology II*, A. Demchenko Eds., Springer, Berlin-Heidelberg (2010).
26. D. Tarn, C. E. Ashley, M. Xue, E. C. Carnes, J. I. Zink and C. J. Brinker, *Acc. Chem. Res.*, **46**(3), 792 (2013).
27. H. Mader, X. Li, S. Saleh, M. Link, P. Kele and O. S. Wolfbeis, *Ann. N. Y. Acad. Sci.*, **1130**, 218 (2008).
28. W. Yang, C. G. Zhang, H. Y. Qu, H. H. Yang and J. G. Xu, *Analytica Chimica Acta*, **503**(2), 163 (2004).
29. T. González-García, S. Fernández, E. Lubian, F. Mancin and M. Ferrero, *RSC Adv.*, **6**(38), 31840 (2016).
30. J.-H. Lim, S.-W. Ha and J.-K. Lee, *Bull. Kor. Chem. Soc.*, **33**(3), 1067 (2012).
31. D. Genovese, S. Bonacchi, R. Juris, M. Montalti, L. Prodi, E. Rampazzo and N. Zaccheroni, *Angew. Chem. Int. Ed.*, **52**(23), 5965 (2013).
32. R. Tapec, X. J. Zhao and W. Tan, *J. Nanosci. Nanotechnol.*, **2**(3-4), 405 (2002).
33. J. A. Funel and S. Abele, *Angew. Chem. Int. Ed.*, **52**(14), 3822 (2013).
34. P. A. Aronov, L. M. Hall, K. Dettmer, C. B. Stephensen and B. D. Hammock, *Anal. Bioanal. Chem.*, **391**(5), 1917 (2008).
35. G. A. Abernethy, *Anal. Bioanal. Chem.*, **403**(5), 1433 (2012).
36. Ž. T. Rakuša, M. Pišlar, A. Kristl and R. Roška, *Pharmaceutics*, **13**(5), 617 (2021).